IEEE Access
Multidisciplinary ⋮ Rapid Review ⋮ Open Access Journal

Received December 4, 2020, accepted December 28, 2020, date of publication December 31, 2020, date of current version January 6, 2021.

*Digital Object Identifier 10.1109/ACCESS.2020.3048519*

# Hybrid Local General Regression Neural Network and Harmony Search Algorithm for Electricity Price Forecasting

**EHAB E. ELATTAR[1,2], (Senior Member, IEEE), SALAH K. ELSAYED[1,3], AND TAMER AHMED FARRAG[4]**

[1]Department of Electrical Engineering, College of Engineering, Taif University, Taif 21944, Saudi Arabia
[2]Department of Electrical Engineering, Faculty of Engineering, Menoufia University, Shebin El-Kom 32511, Egypt
[3]Department of Electrical Engineering, Faculty of Engineering, AL-Azhar University, Cairo 11651, Egypt
[4]Department of Communication and Computer, MISR Higher Institute for Engineering and Technology, Mansoura 35511, Egypt

Corresponding author: Ehab E. Elattar (e.elattar@tu.edu.sa)

This work was supported by Taif University Researchers Supporting Project number (TURSP-2020/86), Taif University, Taif, Saudi Arabia.

**ABSTRACT** Proposing a new precise price forecasting method is still a challenging task as electricity price signals generally exhibit various complex features. In this paper, a new approach for electricity price forecasting called hybrid local general regression neural network, and harmony search algorithm (LGRNN-HSA) is proposed. The proposed LGRNN-HSA is developed by combining the coordinate delay (CD) method, local forecasting paradigm, general regression neural network (GRNN) and harmony search algorithm (HSA). The CD is employed in the proposed method to reconstruct the time series dataset. Then the local forecasting paradigm is utilized with GRNN to predict the future price based on the nearest neighbours only so that the shortcomings in global forecasting methods can be overcome. To enhance the forecasting accuracy, the HSA is employed to optimize not only the parameters of local forecasting paradigm but also the smooth parameter which has a great effect on the accuracy of GRNN. In LGRNN-HSA, a different smooth parameter for every training point is utilized instead of utilizing a constant value in GRNN. To verify the forecasting accuracy of the LGRNN-HSA, a real-world price and demand dataset is employed. The simulation results prove that the LGRNN-HSA significantly improved forecasting accuracy compared to other methods.

**INDEX TERMS** Electricity price forecasting, local forecasting, harmony search algorithm, general regression neural network, parameters optimization.

## NOMENCLATURE

| | |
|---|---|
| $x(t)$ | a time series for $t = 1, 2, \ldots, n$ |
| $n$ | the size of the time series |
| $r(t)$ | embedded vector of $x(t)$ |
| $em$ | the embedding dimension |
| $d$ | the delay constant |
| $x_j(t)$ | a multivariate time series for ($j = 1, 2, \ldots, N$) |
| $N$ | number of time series |
| $em_j$ | the embedding dimension of the $j^{th}$ time series |
| $d_j$ | the time delay constant of the $j^{th}$ time series |
| $L$ | the length of the embedded points produced from reconstruction |
| $f(v, u)$ | the joint probability density function |
| $v$, $u$ | vector random variable and scalar random variable, respectively |
| $v_r$ | particular measured value of $v$ |
| $g$ | dimension of $v$ |
| $\widehat{u}(v_r)$ | the forecasted value of $v_r$ |
| $\sigma$ | smooth parameter |
| $x_i^j$ | harmony vector of decision variables where $i = 1, \ldots, M$ and $j = 1, \ldots, HMS$ |
| $M$ | dimension of the problem |
| $x_{lb,i}$ | lower limit for the decision variables |
| $x_{ub,i}$ | upper limit for the decision variables |
| $r$, $r2$, $r3$, $r3$ | random numbers from 0 to 1 |
| $\overline{O}(t)$ | normalized value at time $t$ |
| $O$ | the value to be normalized at time $t$ |
| $\widehat{EP}_h$ | forecasted EP at hour $h$ |
| $EP_h$ | actual EP at hour $h$ |
| $N_p$ | number of forecasted hours |

The associate editor coordinating the review of this manuscript and approving it for publication was Ahmed A. Zaki Diab.

## I. INTRODUCTION

Throughout, the previous years, electric power markets have faced significant changes. The energy liberalization in several countries in the world dissolved a unified market and converted it into a deregulated competitive one. The electric power market got considerable interest from research over the last few years [1]–[3]. Proposing accurate forecasting methods of the electricity price (EP) is very difficult due to the unique electric price features for instance high-frequency, non- linearity performance and seasonality, climatic variables, high volatility, a high percentage of unusual prices, plus the influence of renewable energy resources [4]–[6]. This makes the price forecasting procedure a challenging job for the researchers [7].

Similar to load forecasting, electricity prices forecasting (EPF) can be categorized into short-term (up to a few days), medium-term (from few weeks up to a year) and long term (over a year and more). This work focuses on short term EPF due to its importance in real-time circumstances. EPF can be employed for several objectives, such as estimation, derivative pricing, and risk management. EPF ensures robust, balanced, and adequately organized operation of the electric power market. Using precise short-term EPF, not only the energy providers can create their tendering policies to increase their settlement plus attain the most significant gain, but also the customers can reduce its consumption fee [8].

In the last few years, numerous forecasting methods for short-term EPF have been presented, specifically conventional and artificial intelligence (AI)-based algorithms. The conventional methods involve autoregressive integrated moving average (ARIMA) [9], [10], wavelet-ARIMA [11] and autoregressive moving average hilbertian (ARMAHX) [12]. However, the conventional methods are appropriately established to get good quality achievement; they are not able to continually characterize the non-linear features of the complicated EP signal. Besides, these algorithms need plenty of data as well as suffer from high computational time.

The AI-based approaches can well suit the nonlinear data and have demonstrated good forecasting results in different applications [13]–[15]. The AI-based approaches have the ability to deal with the non-linear relation between the price signal and its affecting factors; hence the forecasting accuracy is increased.

Various AI methods have been presented in the literature to precisely forecast the EP. In [16], a k-factor GIGARCH procedure has been presented to forecast the electricity price in German. The artificial neural network (ANN) is applied in [17] to forecast both load and price. ANN method has also been applied to forecast the next-week prices in both California and Spanish electricity markets [18]. The traditional ANNs create a nonlinear connection between output and input via a considerable number of historical data. Also, they demonstrate inadequate accuracy for EPF, where they change the dynamic time modelling problem into a static space modelling problem. However the price signal has dynamic characteristics [19]. Different types of ANN are also used to precisely forecast the electricity price, such as deep learning (DL)-based methods, long-short term memory (LSTM) and convolutional neural network (CNN) [20]–[22]. The results of these published papers show the superiority of different ANN types over traditional methods.

One of other popular methods is support vector regression (SVR), which has increased in popularity in the last decades [23]–[25]. The SVR method is employed to predict the electricity price [26], which determines the uncertainty via forecasting the limits of aimed quantities. Also, local informative vector machine (LIVM) is proposed in [8] to forecast electricity price precisely. The merit of SVR comes from replacing the empirical risk minimization principle employed in ANN by structural risk minimization principle. However, SVR has a significant problem where there is a lacking of structural processing for choosing its parameters effectively. Besides as an alternative of forecasting the upcoming EP, there is a concern in assessing the uncertainty engaged in that particular price [27].

Another type of ANN that depends on statistical assumption with kernel regression is the general regression neural network (GRNN) [28]. The significant merits of GRNN in comparison with other ANN forms include precise function estimation from sparse data, quick training actions with straightforward network design, and robustness to both noise and outliers [29]. The authors in [30] applied GRNN with principal components analysis (PCA) to solve the problem of day-ahead EPF. Where, PCA is employed to avoid a significant correlation among the input factors that may affect electricity price.

Instead of using the above methods solely, two or more methods are combined together or with other optimization approaches to get better results for EPF. The hybrid backtracking search algorithm and adaptive neuro-fuzzy inference system (ANFIS) method is proposed in [31] to precisely forecast electricity price. Also, the authors in [32] presented the ensemble of relevance vector machines with boosted trees to predict electricity locational marginal price. Besides, an optimized heterogeneous structure LSTM is proposed in [19] to solve the EPF problem. Moreover, a prototype asymmetric-based neuro-fuzzy network (AGFINN) is presented for short-term EPF based on the data from new England market [33]. The authors in [34] combined daily pattern prediction with classification modelling approach for DAEPF is proposed to solve the problem of unified modelling of the data which gives a large error in EPF. The enhanced convolutional neural network and enhanced SVR are also proposed in [35] for EPF and load forecasting the smart grid, where grid search is employed for tuning their parameters to enhance their forecasting ability. The dynamic choice ANN for EPF is proposed in [36] where the index of bad samples matrix which dynamically confirm bad training samples and optimization algorithm are combined with the algorithm to enhance its forecasting accuracy.

An essential aspect that affects the accuracy and ability forecasting of the electricity price is feature selection. The authors in [31] proposed a multi-objective feature selection procedure consist of a multi-objective binary-valued backtracking search and ANFIS algorithm to obtain the most relevant subgroups of inputs with less redundancy. A mixture of a feature selection procedure with a cascaded neuro-evolutionary algorithm is presented in [37] for EPF. ANN and stage selection feature system are integrated in [38] to improve the price forecasting accuracy. Appropriate choice of features can improve the efficiency and accuracy of load and EPF [39]. But it is incredibly challenging to choose the robust feature selection procedure for EPF taking into account non-linearity of price signal.

The above-discussed methods are identified as a global forecaster in which a forecaster is trained based on all historical points existing or employing a feature selection process to select a suitable training points. These types of forecasters have different downsides which are reviewed and overcome using local forecasters in our previous work [8], [13]–[15].

As a result of the complication and non-linearity of the electricity price signal, the procedure employed in the local forecasters of time-series can be used in EPF. This procedure is called phase space reconstruction. Therefore, the coordinate delay (CD) method is utilized in this work to obtain the embedding dimension and the time delay of the electricity price signal.

Although various methods have been proposed and employed for EPF, none of them consistently gives precise forecasts. Consequently, a more effective EPF framework is necessary because many markets members and system operators rely on it. So, a hybrid local GRNN (LGRNN) and harmony search algorithm (HSA) is proposed in this work. Choosing the smooth parameter has a high effect on the forecasting ability of the GRNN. A solo value of this parameter may not commonly give an optimum configuration. Hence, a separate smooth parameter for each training data which optimally chosen by HSA, will be used in this work to obtain a superior control of the regression surface's smoothness. The HSA not only employed to choose the optimal values of the smooth parameter but also utilized to find the optimal values of the embedding dimension, the time delay constant, and the number of nearest neighbors of the local forecasting paradigm. To investigate the precision of the proposed hybrid method, the electricity price dataset from the Ontario electricity market is used. The Ontario electricity market is identified as an unbalanced markets owing to its single agreement nature [40], [41]. Thus, it gives a considerable challenge in the prediction of its EP. The contributions of this work are:

- Proposing a hybrid EPF method to get extra precise forecasts via employing an efficient HSA with LGRNN approach. The HSA is utilized in the hybrid method to enhance the forecasting accuracy of LGRNN by optimally choosing the smooth parameter and local forecasting paradigm's parameters. HSA is employed because of the simplicity and its effectiveness in solving different optimization problems.
- The local forecaster method-based GRNN, which employs various bandwidths integrated with space reconstruction of electricity price signal, is presented. Where a separate smooth parameter for each training data is presented in the LGRNN method instead of using a fixed smooth parameter in the conventional GRNN.
- The hybrid method is tested carefully by comparing it with other published approaches based on the real world dataset.
- Enhancing EPF accuracy in comparison with the results taken from other forecasting methods.

## II. OVERVIEW OF LOCAL GENERAL REGRESSION NEURAL NETWORK (LGRNN) AND HSA

### A. TIME-SERIES RECONSTRUCTION

A frequently employed method for the analysis of complicated time series is the phase space reconstruction method, which is extracted from the embedding theorem presented in [42], [43]. Suppose there is a time series $x(t)$ and according to the embedding theorem, it can be expanding as follows:

$$r(t)=[x(t), x(t-d), x(t-2d), \ldots, x(t-(em-1)d)] \quad (1)$$

The two important parameters in phase space reconstruction are $em$ and $d$ are calculated in this work using the correlation dimension and the mutual information approaches, respectively.

Corresponding to the embedding theorem the reconstructed vector of n-time series in the phase space could be signified as [44]:

$$r_j(t) = [x_j(t), x_t(t-d_j), x_j(t-2d_j), \ldots, x_j(t-(em_j-1)d_j)] \quad (2)$$

where $L$ can be computed as, $L = n - \max_{j=1,\ldots,N}[(em_j - 1)d_j]$, $r(t)$ is now a $L \times T$ matrix and $T = \sum_{j=1}^{N} em_i$.

The details of employing both the correlation dimension method and mutual information method to get the appropriate values of $em$ and $d$ have been described in [45].

### B. GRNN OVERVIEW

GRNN is a type of nonlinear ANN proposed in [28]. GRNN has a topology look like ANN. But GRNN has some merits in comparison with ANN and SVR. GRNN has fewer adjustment parameters in comparison with ANN and SVR. Also, it does not merely fall into local minima. Besides, it has a good performance while processing large-scale training datasets. Moreover, it has an advantage in forecasting volatile data. GRNN can obtain reasonable solutions in both classification and forecasting problems. The theory of kernel regression is the basis of GRNN operation [46].

Suppose that the joint probability density function of $v$ and $u$ is $f(v, u)$. The regression of $u$ on $v_r$ is given by:

$$\widehat{u}(v_r) = E[u|v_r] = \frac{\int_{-\infty}^{\infty} uf(v_r, u)du}{\int_{-\infty}^{\infty} f(v_r, u)du} \quad (3)$$

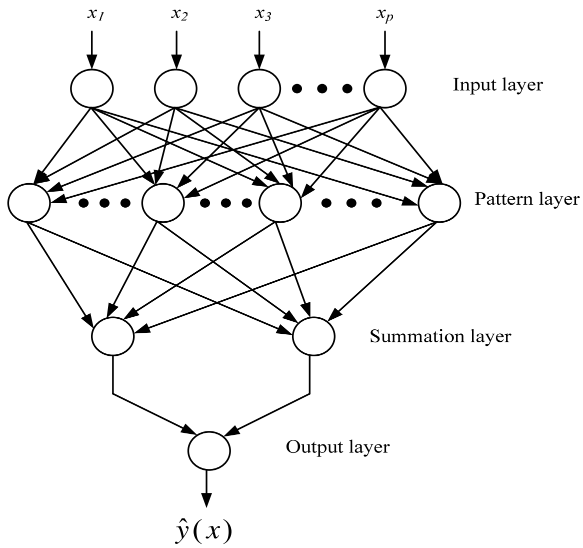


**FIGURE 1.** GRNN architecture.

When $f(v, u)$ is not recognized, it have to typically be calculated from a sample of $v$ and $y$. By employing Parzen distribution free, the function $f(v_r, u)$ can be found based on (3) by sample data collection $\{v_i, u_i\}_{i=1}^n$ ( $v \in \mathcal{R}^g$ is the g-dimensional input vector and $u = f(v) \in \mathcal{R}$ its resultant real-valued output).

$$f(v_r, u) = \frac{1}{n(2\pi)^{\frac{g+1}{2}} w_1 w_2 \dots w_g w_u} \sum_{i=1}^{n} e^{-D(v_r,v_i)} e^{-D(u,u_i)} \tag{4}$$

$$D(v_r, v_i) = \frac{(v_r - v_i)^2}{2\sigma^2}, \quad D(u, u_i) = \frac{(u - u_i)^2}{2\sigma^2} \tag{5}$$

The critical parameter of the GRNN called the smooth parameter ($\sigma$) has a considerable influence on its ability to predict. $\sigma$ establishes the function's broad, which characterizes the area of impact and, hence, the total examples are taken into account to evaluate a variable [47]. For a large value of $\sigma$, further examples will be deemed. Alternatively, if $\sigma$ is quite tiny, a small number of examples are considered.

By replacing (4) into (3), $\widehat{u}(v_r)$ is calculated as:

$$\widehat{u}(v_r) = \frac{\sum_{i=1}^{n} (e^{-D(v_r,v_i)} \int_{-\infty}^{\infty} u e^{-D(u,u_i)} du)}{\sum_{i=1}^{n} (e^{-D(v_r,v_i)} \int_{-\infty}^{\infty} e^{-D(u,u_i)} du)} \tag{6}$$

Solving the two integrals of (6) produces the following:

$$\widehat{u}(v_r) = \frac{\sum_{i=1}^{n} u_i e^{-D(v_r,v_i)}}{\sum_{i=1}^{n} e^{-D(v_r,v_i)}} \tag{7}$$

So the forecasted value $\widehat{u}(v_r)$ is the weighted mean of all of the recorded values $u_i$.

The topology of the GRNNs consists of 4 levels of the processing unit, as indicated in Fig. 1. Every level of these units is designated with a particular function while nonlinear regression is done. More details about GRNN can be extracted from [28]

## *C. LGRNN*

In local forecasters, a set of data called $K$ nearest neighbors extracted from the reconstructed time series are only utilized to forecast the future values. This gives the local forecasters the ability to overcome global forecasters' shortcomings because the global forecasters are employing all historical instances that may be distant and less appropriate. Another advantage of local forecasters is that they split the domain into several subsections (neighborhoods). Consequently, the dynamic features of the dataset are studied gradually and locally in the reconstructed space. Also, the training window employed for each query point in the local forecaster is considerably smaller than the global forecasters where much historical data is utilized for training the model. This reduces the overall computational time and memory space for the local forecasters [8], [13].

To construct the local forecaster, two aspects have to be determined. These aspects are the suitable number of $K$ and the way of selecting them. In this work, the nearest neighbors are selected based on the Euclidean distance, while the appropriate number of $K$ is optimized using HSA.

Overall, there are 4 main steps in the construction of the LGRNN. The LGRNN begins with the reconstruction of the given dataset. Then the nearest neighbors ($K$) are chosen for every query data point. After that, the procedures of GRNN are implemented based on $K$ only. In the last step, GRNN is evaluated based on the query data point to assess the process output.

## *D. HSA*

The meta-heuristic harmony search algorithm (HSA) is inspired from the musical improvisation process [48]. The HSA has various features. It requires a small number of mathematical requirements and decreases the number of iterations necessary to get the optimal solution. Also, it employs stochastic random searches, so the derivative information is unwarranted. A musician represents every decision variable in the optimization problem. Then every musician performs a note (produce a value) to get the finest harmony (global optimal) [48]. The HSA is simple to implement; however, it has some parameters that need to be determined. Its applications in different optimization problems give better performance compared to other different meta-heuristic algorithms [49], [50].

The parameters of the HSA which adjusted at the beginning of the algorithm are the size of harmony memory (HMS), harmony memory considering rate (HMCR), pitch adjusting rate (PAR) and bandwidth (BW). In the second step, an initial population of harmonies (solutions) is produced randomly and stored corresponding to their fitness in the harmony memory (HM). The initial HM is created using the following equation:

$$x_i^j = x_{lb,i} + r * (x_{ub,i} - x_{lb,i}) \tag{8}$$

$$HM = \begin{bmatrix} x_1^1 & x_2^1 & \ldots & x_M^1) \\ x_1^2 & x_2^2 & \ldots & x_M^2) \\ \ldots & \ldots & \ldots & \ldots \\ x_1^{HMS} & x_2^{HMS} & \ldots & x_M^{HMS}) \end{bmatrix} \quad (9)$$

In the third step, which is the most important one, a new harmony (solution) is created from the stored harmonies in HM using any mixture of the three different rules. The first one is "memory consideration" that makes use of accumulative search. The second rule is "random initialization" to diversify the new harmony. The last rule is "pitch adjustment" to be similar to a local search. At the beginning, the parameter HMCR ($HMCR \in [0, 1]$) is utilized to chose a new value. HMCR determines whether the new value is chosen to form the HM's stored values (if $HMCR \geq r2$) or randomly created from the feasible range of the decision variables if ($HMCR < r2$):

$$x_i' = \begin{cases} x_i' \in \{x_i^1, x_i^2, \ldots, x_i^{HMS}\} & HMCR \geq r2 \\ x_i' \in [x_{lb,i}, x_{ub,i}] & \text{otherwise} \end{cases} \quad (10)$$

Then, each harmony vector selected from HM is examined to decide whether it would be pitch-adjusted based on the PAR parameter as follows:

$$\text{Pitch-adjusting rule for} x_i' = \begin{cases} \text{Yes} & PAR \geq r3 \\ \text{No} & \text{otherwise} \end{cases} \quad (11)$$

If the decision is yes for any $x_i'$, the $x_i'$ value is updated as follows:

$$x_i' = x_i' + r4 \times BW \quad (12)$$

The new harmony is assessed in the fourth step and HM is revised by replacing its worst harmony (solution) with the new one. Lastly, the above procedures are repeated until the stopping criterion is met. The details of HSA can be found in [48]–[50].

## III. PRICE FORECASTING BASED ON HYBRID LGRNN AND HSA

The parameter $\sigma$ has a massive impact on the forecasting precession of GRNN. It is hard to calculate the parameter $\sigma$ precisely. So, different optimization techniques usually employed to optimally chose this parameter [46]. Choosing this parameter as a large value increases the spread of the Gaussian distribution curve. On the contrary, a small value of $\sigma$ makes the curve more compact. For moderate $\sigma$, all sample observed value are considered although those related to patterns nearer to the sample observed value are provided larger weight.

A single value of $\sigma$ is utilized in In [28] for the whole input variables. But utilizing a single value for all variables may not commonly give an optimal configuration, as the time series might have dissimilar densities in different zones of input space. To overcome this drawback, the HSA is employed in this work to get the precise value of $\sigma$, where a different value of $\sigma$ per training data will be utilized. Besides, the HSA is also utilized to optimally determine the proper values of the two essential parameters of the CD method (the embedding dimension and the time delay constant).

The main steps of the proposed hybrid LGRNN and HSA can be summarized as follows:

- $1^{st}$ step: Load the multivariate time series data and set the parameters of HSA.
- $2^{nd}$ step: For each query point, generate the initial population. Each harmony vector consists of the values of smooth parameter, embedding dimension, time delay constant, and K. These vectors are all randomly initialized.
- $3^{rd}$ step: Applying the CD method to reconstruct the multivariate time series data.
- $4^{th}$ step: Applying the local forecasting paradigm by choosing the K nearest neighbours for the current query point using the Euclidean distance
- $5^{th}$ step: The HSA is employed in this step where the best harmony vector in the last generation represents the optimal parameters.
- $6^{th}$ step: The GRNN is utilized in this step based on the optimized parameters to calculate the current query's prediction value.
- $7^{th}$ step: Steps 2 to 6 can be repeated till the forecasted values of various query points are all obtained.

The overall process of the proposed hybrid LGRNN and HSA applied to EPF is indicated by the flowchart shown in Fig. 2.

## IV. SIMULATION RESULTS

In the deregulated electricity market, EP is a function of electricity load. This means that the EP at any time rely on the electrical load as well as the historical values of electricity load and price. The proposed LGRNN-HSA algorithm is presented in this work to forecast the hourly EP of Ontario based on the load and price historical values in 2017 [22]. Also, the historical data is normalized based on (13) [31] because of the broad range of historical values.

$$\overline{O}(t) = \frac{O(t) - min(O)}{max(O) - min(O)} + 1 \quad (13)$$

Besides, to prove the superiority of the LGRNN-HSA algorithm over other methods, the achieved results are compared with the results of LGRNN, ARIMA, wavelet ARIMA, and the approaches published in [31]. These approaches are ANN, ANFIS, ANN with genetic algorithm (ANN-GA), ANN with particle swarm algorithm (ANN-PSO), ANFISGA, ANN with backtracking search algorithm (ANN-BSA), ANFIS-PSO, and ANFIS-BSA.

For a fair comparison with the methods published in [31], hourly load and price historical values are employed. Also, the same four months representing different seasons are employed. These months are February (winter season), May (spring season), August (summer season), and November (fall season). The historical values of the first three weeks of each month are utilized for training and the fourth week is

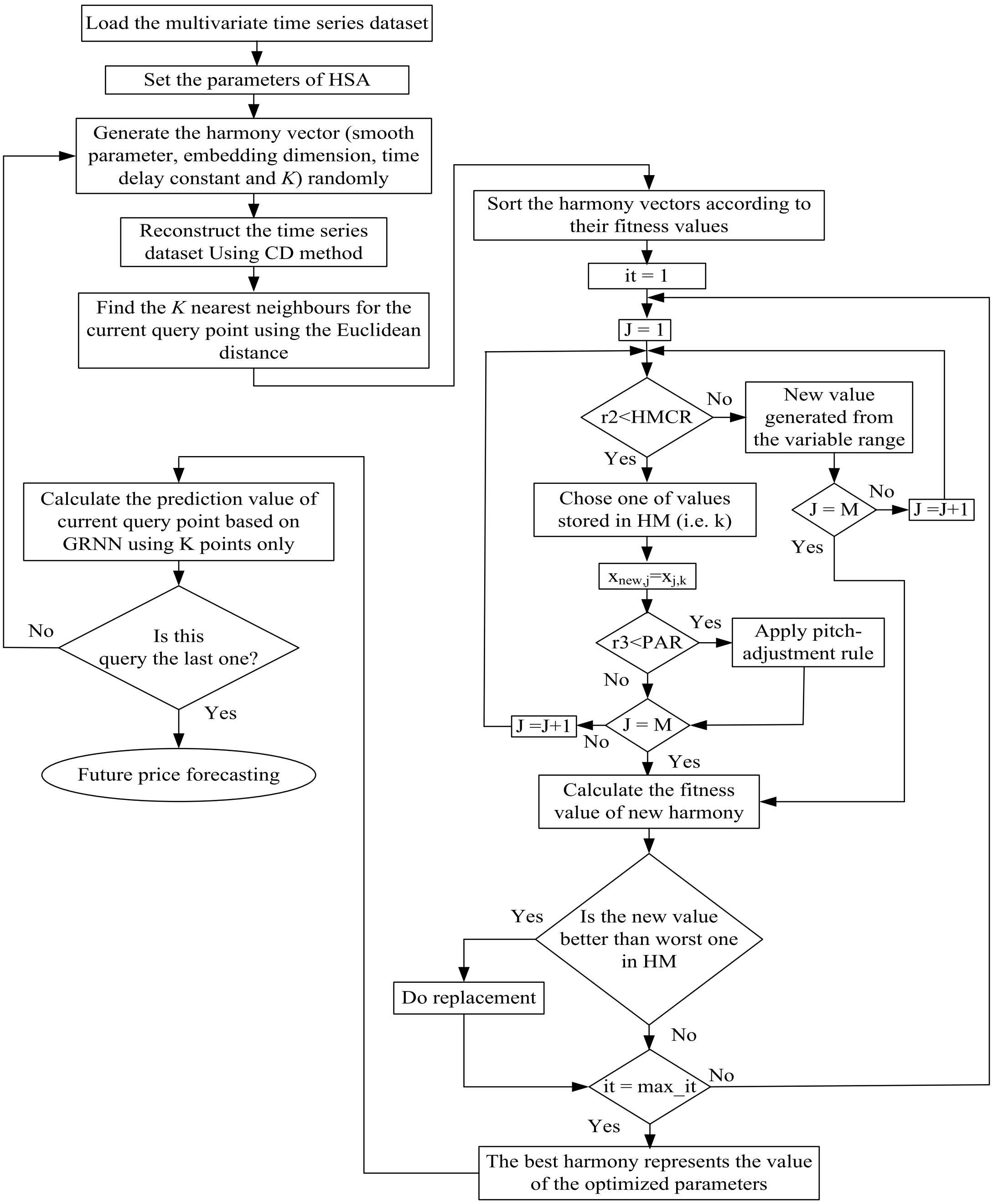


**FIGURE 2.** Flowchart of the hybrid LGRNN and HSA.

employed for testing. The details of training and testing data are tabulated in table 1. The parameters of LGRNN-HSA are: HMS = 30, HMCR = 0.9, PAR = 0.1, and BW = 0.02. All the numerical studies are carried out on 2.8-GHz i7 PC with 16 GB of RAM using MATLAB 2020a.

### A. FORECASTING ACCURACY EVALUATION

Like [31], the mean absolute percentage error (MAPE), root mean square error (RMSE), and thiel's inequality coefficient (U-statistic) are employed in this work to assess the accuracy of the lGRNN-HSA in forecasting EP.

$$\mathrm{MAPE} = \frac{1}{N_p}\sum_{h=1}^{N_p}\frac{|\widehat{EP}_h - EP_h|}{EP_h} \times 100 \tag{14}$$

$$\mathrm{RMSE} = \sqrt{\frac{1}{N_p}\sum_{h=1}^{N_p}[\widehat{EP}_h - EP_h]^2} \tag{15}$$

$$U = \frac{RMSE}{\sqrt{\frac{1}{N_p}\sum_{h=1}^{N_p} EP_h^2} + \sqrt{\frac{1}{N_p}\sum_{h=1}^{N_p} \widehat{EP}_h^2}} \tag{16}$$

**TABLE 1.** The data used for forecasting models for training and testing.

| Season | Historical hourly values | Test week | Number of samples | |
|---|---|---|---|---|
| | | | Training data | Testing data |
| Winter | Feb. 1 to Feb. 21 | Feb. 22 to Feb. 28 | 504 | 168 |
| Spring | May 1 to May 24 | May 25 to May 31 | 576 | 168 |
| Summer | Aug. 1 to Aug. 24 | Aug. 25 to Aug. 31 | 576 | 168 |
| Fall | Nov. 1 to Nov. 23 | Nov. 24 to Nov. 30 | 552 | 168 |

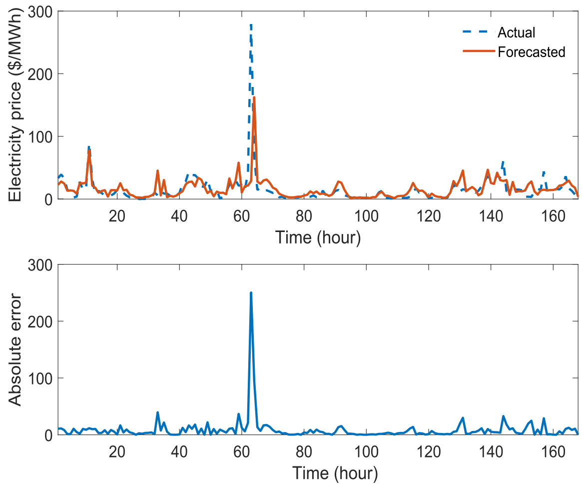


**FIGURE 3.** The performance of LGRNN-HSA during winter test week (Feb. 2017) and its corresponding absolute error.

## B. RESULTS

Figure 3 shows the performance of the proposed LGRNN-HSA method of Ontario in the winter test week (February 2017). Where the comparison between the forecasted price values and the actual values as well as the absolute error ($|Forecasted - actual|$) values are indicated in the figure. One can notice that that the EPF values of the winter test week are precisely similar to the real price values.

The results of the LGRNN-HSA, LGRNN, ARIMA, wavelet ARIMA, and the methods published in [31] for the winter test week (Feb. 2017) are shown in Table 2. According to these results, the LGRNN-HSA method has the best accuracy in EPF, amongst other methods. The LGRNN-HSA improves the MAPE over LGRNN by 15.05% while it reduces the MAPE of ANFIS-BSA (the best algorithm after the proposed one) by 12.21%.

The performance of the proposed LGRNN-HSA method in the spring test week (May 2017) is indicated in Figure 4, which gives the comparison between the forecasted price values and the actual values as well as the absolute error. The results obviously indicate that the proposed method can obtain forecasted EP values close to the real price values. Besides, Table 3 indicates the obtained results of all studied algorithms for the spring test week (May 2017). Again, the results reveal that the LGRNN-HSA method has the best accuracy in EPF, amongst other methods. The LGRNN-HSA improves the MAPE over LGRNN by 19.04% while it reduces the MAPE of ANFIS-BSA (the best algorithm after the proposed one) by 6.81%.

The comparison between the forecasted and actual price in the summer test week (August 2017) using the LGRNN-HSA method is shown in Figure 5 which also shows the absolute

**TABLE 2.** Comparison between the results of all studied methods in winter test week (Feb. 2017).

| Methods | Performance index | | |
|---|---|---|---|
| | RMSE | U-statistic | MAPE (\%) |
| ARIMA | 0.0935 | 0.0475 | 5.2113 |
| Wavelet ARIMA | 0.0821 | 0.0399 | 4.4589 |
| ANN [31] | 0.0867 | 0.0411 | 4.8865 |
| ANN-GA [31] | 0.0812 | 0.0396 | 4.4445 |
| ANN-PSO [31] | 0.0802 | 0.0384 | 4.2347 |
| ANN-BSA [31] | 0.0775 | 0.0346 | 3.7654 |
| ANFIS [31] | 0.0798 | 0.0386 | 4.7899 |
| ANFIS-GA [31] | 0.0734 | 0.0332 | 3.0643 |
| ANFIS-PSO [31] | 0.0678 | 0.0309 | 2.7647 |
| ANFIS-BSA [31] | 0.0628 | 0.0297 | 2.5237 |
| LGRNN | 0.0683 | 0.0310 | 2.6080 |
| LGRNN-HSA | 0.0620 | 0.0222 | 2.2155 |

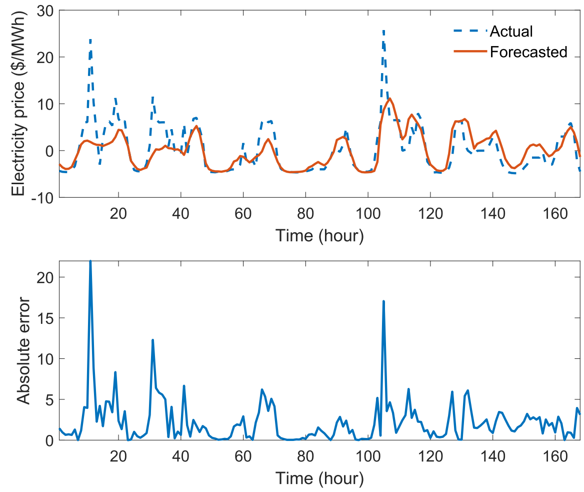


**FIGURE 4.** The performance of LGRNN-HSA during spring test week (May 2017) and its corresponding absolute error.

**TABLE 3.** Comparison between the results of all studied methods in spring test week (May 2017).

| Methods | Performance index | | |
|---|---|---|---|
| | RMSE | U-statistic | MAPE (\%) |
| ARIMA | 0.0287 | 0.0112 | 1.2301 |
| Wavelet ARIMA | 0.0223 | 0.0101 | 0.9999 |
| ANN [31] | 0.0245 | 0.0107 | 1.1397 |
| ANN-GA [31] | 0.0244 | 0.0092 | 1.1014 |
| ANN-PSO [31] | 0.0229 | 0.0082 | 1.0009 |
| ANN-BSA [31] | 0.0194 | 0.0077 | 0.9879 |
| ANFIS [31] | 0.0251 | 0.0089 | 1.1165 |
| ANFIS-GA [31] | 0.0178 | 0.0069 | 0.8963 |
| ANFIS-PSO [31] | 0.0201 | 0.0071 | 0.9181 |
| ANFIS-BSA [31] | 0.0133 | 0.0065 | 0.7957 |
| LGRNN | 0.0139 | 0.0075 | 0.9160 |
| LGRNN-HSA | 0.0123 | 0.0064 | 0.7415 |

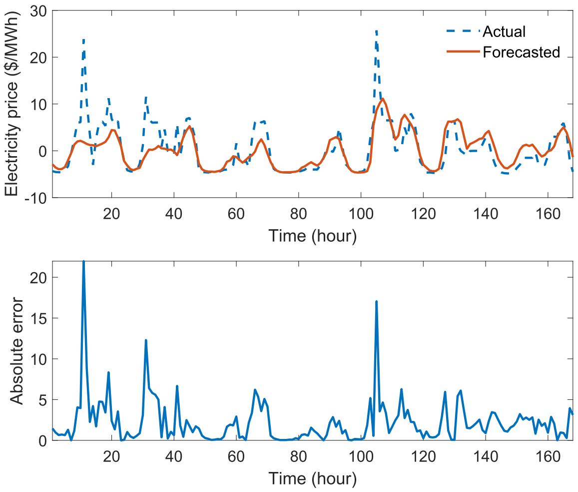


**FIGURE 5. The performance of LGRNN-HSA during spring test week (May 2017) and its corresponding absolute error.**

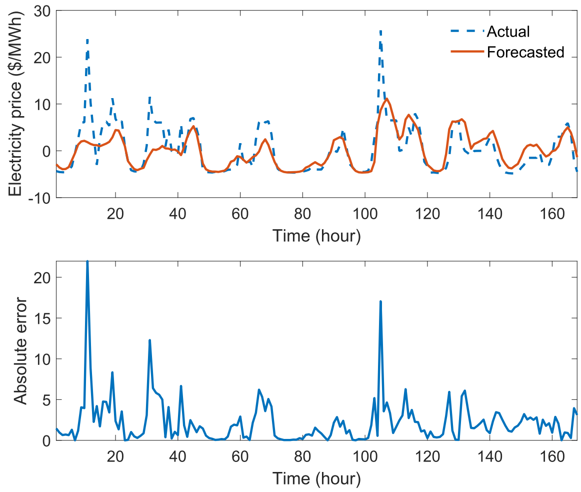


**FIGURE 6. The performance of LGRNN-HSA during spring test week (May 2017) and its corresponding absolute error.**

**TABLE 4. Comparison between the results of all studied methods in summer test week (August 2017).**

| Methods | Performance index | | |
|---|---|---|---|
| | RMSE | U-statistic | MAPE (\%) |
| ARIMA | 0.0397 | 0.0202 | 2.9101 |
| Wavelet ARIMA | 0.0345 | 0.0181 | 2.4591 |
| ANN [31] | 0.0357 | 0.0198 | 2.6543 |
| ANN-GA [31] | 0.0345 | 0.0188 | 2.5328 |
| ANN-PSO [31] | 0.0312 | 0.0178 | 2.3456 |
| ANN-BSA [31] | 0.0323 | 0.0185 | 2.4538 |
| ANFIS [31] | 0.0337 | 0.0189 | 2.2456 |
| ANFIS-GA [31] | 0.0278 | 0.0132 | 1.9643 |
| ANFIS-PSO [31] | 0.0254 | 0.1150 | 1.7632 |
| ANFIS-BSA [31] | 0.0223 | 0.0102 | 1.4117 |
| LGRNN | 0.0243 | 0.0115 | 1.5001 |
| LGRNN-HSA | 0.0183 | 0.0099 | 1.3213 |

**TABLE 5. Comparison between the results of all studied methods in fall test week (November 2017).**

| Methods | Performance index | | |
|---|---|---|---|
| | RMSE | U-statistic | MAPE (\%) |
| ARIMA | 0.0822 | 0.0504 | 4.3338 |
| Wavelet ARIMA | 0.0746 | 0.0452 | 4.0318 |
| ANN [31] | 0.0794 | 0.0497 | 4.0428 |
| ANN-GA [31] | 0.0743 | 0.0478 | 3.9797 |
| ANN-PSO [31] | 0.0720 | 0.0463 | 3.8346 |
| ANN-BSA [31] | 0.0701 | 0.0456 | 3.7543 |
| ANFIS [31] | 0.0785 | 0.0482 | 3.8203 |
| ANFIS-GA [31] | 0.0676 | 0.0451 | 3.3451 |
| ANFIS-PSO [31] | 0.0503 | 0.0389 | 2.7521 |
| ANFIS-BSA [31] | 0.0431 | 0.0358 | 2.4180 |
| LGRNN | 0.0467 | 0.0311 | 2.5439 |
| LGRNN-HSA | 0.0416 | 0.0218 | 2.3716 |

error of the LGRNN-HSA method. Again, the results indicate that the proposed method can obtain forecasted EP values close to real price values. In addition, Table 4 indicates the obtained results of all studied algorithms for the summer test week (May 2017). These results prove the effectiveness of the LGRNN-HSA over other studied algorithms. The LGRNN-HSA reduces the MAPE over LGRNN and ANFIS-BSA (the best algorithm after the proposed one) by 11.92% and 6.40%, respectively.

Figure 6 shows the comparison between the forecasted and actual price in the fall test week (November 2017) using the LGRNN-HSA method which also indicates the absolute error of the LGRNN-HSA method. As in the previous test weeks, the results show that the LGRNN-HSA can obtain forecasted EP values close to actual values. Also, Table 5 shows the obtained results of all studied algorithms for the fall test week (November 2017). These results demonstrate the superiority of the LGRNN-HSA over other studied algorithms. The LGRNN-HSA reduces the MAPE over LGRNN and ANFIS-BSA (the best algorithm after the proposed one) by 6.77% and 1.92%, respectively. Figure 7 shows the comparison between the daily MAPE values of LGRNN-HSA and LGRNN algorithms for the four test weeks which ensure the superiority of the LGRNN-HSA over LGRNN.

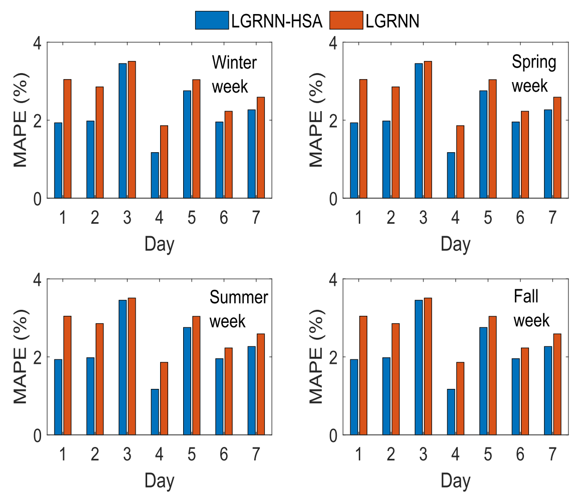


**FIGURE 7. Daily MAPE values of LGRNN-HSA and LGRNN algorithms for all test weeks.**

**TABLE 6. Improvement of the LGRNN-HSA over other algorithms based on the average MAPE, U-statistic, and RMSE.**

| | MAPE (%) | | U-statistic | | RMSE | |
|---|---|---|---|---|---|---|
| Methods | Average | Improvement (%) | Average | Improvement (%) | Average | Improvement (%) |
| LGRNN-HSA | 1.6625 | | 0.0151 | | 0.0336 | |
| ARIMA | 3.4213 | 51.4086 | 0.0323 | 53.3031 | 0.0610 | 45.0272 |
| Wavelet ARIMA | 2.9874 | 44.3510 | 0.0283 | 46.6944 | 0.0534 | 37.1821 |
| ANN [31] | 3.1808 | 47.7350 | 0.0303 | 50.2557 | 0.0566 | 40.6886 |
| ANN-GA [31] | 3.0146 | 44.8531 | 0.0289 | 47.7125 | 0.0536 | 37.3966 |
| ANN-PSO [31] | 2.8540 | 41.7489 | 0.0277 | 45.4925 | 0.0516 | 34.9386 |
| ANN-BSA [31] | 2.7404 | 39.3341 | 0.0266 | 43.2896 | 0.0498 | 32.6534 |
| ANFIS [31] | 2.9931 | 44.4565 | 0.0287 | 47.3475 | 0.0543 | 38.1752 |
| ANFIS-GA [31] | 2.3175 | 28.2650 | 0.0246 | 38.6791 | 0.0467 | 28.0698 |
| ANFIS-PSO [31] | 2.0495 | 18.8857 | 0.0480 | 68.5566 | 0.0409 | 17.9574 |
| ANFIS-BSA [31] | 1.7873 | 6.9836 | 0.0206 | 26.5939 | 0.0354 | 5.1437 |
| LGRNN | 1.8920 | 12.1322 | 0.0203 | 25.6074 | 0.0383 | 12.3879 |

**TABLE 7. Wilcoxon signed-rank test.**

| | $\alpha = 0.025$ W = 0 | $\alpha = 0.05$ W = 0 |
|---|---|---|
| LGRNN-HSA vs. ARIMA | 0 | 0 |
| LGRNN-HSA vs. Wavelet ARIMA | 0 | 0 |
| LGRNN-HSA vs. LGRNN | 0 | 0 |

### C. DISCUSSION

The obtained results of the proposed LGRNN-HSA method for four test weeks are compared with different published algorithms using the same conditions for a fair comparison. These comparisons confirm the superiority of LGRNN-HSA over other studied algorithms in the four test weeks. Table 6 shows the average MAPE, average U-statistic, and average RMSE of all methods for the four test weeks as well as the improvement of the LGRNN-HSA over other algorithms. The results demonstrate the capability of the LGRNN-HSA method to obtain a better EPF solution for different seasons. This capability is due to employing the local forecasting paradigm which overcomes the drawbacks of the global methods. Also, by optimizing the parameters of the local forecasting paradigm and GRNN's smooth parameters which enhance the forecasting accuracy over LGRNN, where its parameters are chosen using the cross-validation method.

U-statistic is an index to display how properly-fitted a time series of predicted values are to a consequent time series of real data. The value of this index usually varies from 0 to 1. The closer to zero, the more accurate forecasting is achieved with a perfect fit. Thus, the closer to 1, the less accuracy in the forecasting value. As indicated from the previous results of the four test weeks, the U-statistic values of the proposed LGRNN-HSA are closer to 0 than other studied approaches. This proves that more accurate forecasting can be obtained using LGRNN-HSA compared to other studied techniques.

Additionally, to confirm the significance of the forecasting accuracy of the proposed LGRNN-HSA over ARIMA, wavelet ARIMA, and LGRNN in the four testing weeks, two statistical tests are conducted. They are the Mann-Whitney U test [51] and Wilcoxon signed-rank test [52]. The Mann-Whitney U test is performed at the 0.05 significance levels in a one-tailed test. The P values for (LGRNN-HSA versus ARIMA), (LGRNN-HSA versus wavelet ARIMA), and (LGRNN-HSA versus LGRNN) are 0.0021, 0.0029, and 0.0071, respectively, which is less than 0.05. These results indicate that the LGRNN-HSA gives considerably better forecast results than other approaches. The Wilcoxon signed-rank test is performed at the 0.025 and 0.05 significance levels in one-tail tests. Table 7 indicates the results of this statistical test which prove the forecasting significance of the LGRNN-HSA over other compared approaches.

Figure 8 shows the MAPE's convergence characteristics of the LGRNN-HSA for the four test weeks. This figure indicates that the MAPE converges efficiently to the optimum value without any abrupt fluctuations that demonstrate the convergence reliability of the LGRNN-HSA.

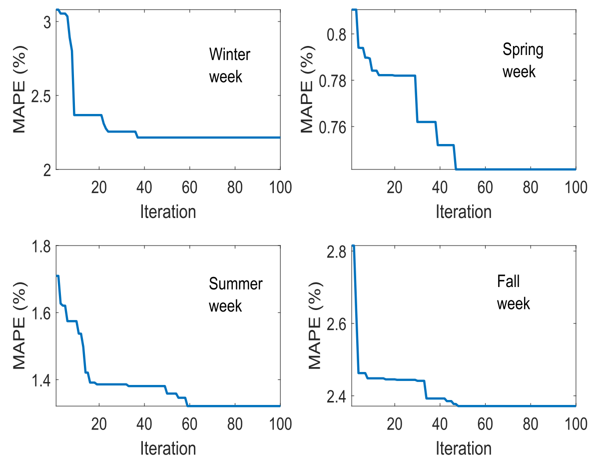


**FIGURE 8. Convergence characteristics of the proposed method for the four test weeks.**

**TABLE 8. Statistical test of the LGRNN-HSA for the four test weeks based on MAPE.**

| | Minmum | Median | Maximum | SD |
|---|---|---|---|---|
| Winter week | 2.2155 | 2.2445 | 2.4045 | 0.0772 |
| Spring week | 0.7415 | 0.7889 | 0.8652 | 0.0346 |
| Summer week | 1.3213 | 1.375 | 1.4528 | 0.0594 |
| Fall week | 2.3716 | 2.3716 | 2.3949 | 0.0074 |

To check the robustness of the LGRNN-HSA, 20 separate runs are carried out for the four test weeks. Then the minimum, the maximum, the median, and the standard deviation (SD) values of the LGRNN-HSA for each test week. These results are presented in Table 8, which reveals that the SD for the four test weeks is tiny, which implies the effectiveness and the robustness of the LGRNN-HSA.

## V. CONCLUSION

In this work, a hybrid algorithm (LGRNN-HSA) is proposed for EPF in the Ontario electricity market. The hybrid proposed algorithm combines the local forecasting paradigm, GRNN and HSA. The local forecasting paradigm helps the proposed algorithm to overcome the demerits of the global algorithms. Besides, the HSA is employed to optimize the local forecasting's parameters as well as the smooth parameter of the GRNN which affects the forecasting capability of the GRNN. A real-world dataset from Ontario is utilized to assess the forecasting ability of the LGRNN-HSA in comparison with some published approaches. The obtained results reveal that the proposed LGRNN-HSA algorithm has a superior forecasting performance in terms of accuracy and robustness compared to other approaches using four test weeks. So, the LGRNN-HSA could be recommended as a robust and effective forecasting tool for utility engineers.

## ACKNOWLEDGMENT

The authors would like to acknowledge the financial support received from Taif University Researchers Supporting Project Number (TURSP-2020/86), Taif University, Taif, Saudi Arabia.

## REFERENCES

[1] I. Shah, H. Bibi, S. Ali, L. Wang, and Z. Yue, "Forecasting one-day-ahead electricity prices for italian electricity market using parametric and nonparametric approaches," *IEEE Access*, vol. 8, pp. 123104–123113, 2020.

[2] P. Muniain and F. Ziel, "Probabilistic forecasting in day-ahead electricity markets: Simulating peak and off-peak prices," *Int. J. Forecasting*, vol. 36, no. 4, pp. 1193–1210, Oct. 2020.

[3] J.-L. Zhang, Y.-J. Zhang, D.-Z. Li, Z.-F. Tan, and J.-F. Ji, "Forecasting day-ahead electricity prices using a new integrated model," *Int. J. Electr. Power Energy Syst.*, vol. 105, pp. 541–548, Feb. 2019.

[4] Z. Yang, L. Ce, and L. Lian, "Electricity price forecasting by a hybrid model, combining wavelet transform, ARMA and kernel-based extreme learning machine methods," *Appl. Energy*, vol. 190, pp. 291–305, Mar. 2017.

[5] K. Maciejowska, "Assessing the impact of renewable energy sources on the electricity price level and variability—A quantile regression approach," *Energy Econ.*, vol. 85, Jan. 2020, Art. no. 104532.

[6] D. Aineto, J. Iranzo-Sánchez, L. G. Lemus-Zñiga, E. Onaindia, and J. F. Urchueguía, "On the influence of renewable energy sources in electricity price forecasting in the iberian market," *Energies*, vol. 12, no. 11, p. 2082, May 2019.

[7] M. Ribeiro, S. Stefenon, J. de Lima, A. Nied, V. Mariani, and L. Coelho, "Electricity price forecasting based on self-adaptive decomposition and heterogeneous ensemble learning," *Energies*, vol. 13, no. 19, p. 5190, Oct. 2020.

[8] E. E. Elattar, "Day-ahead price forecasting of electricity markets based on local informative vector machine," *IET Gener., Transmiss. Distrib.*, vol. 7, no. 10, pp. 1063–1071, Oct. 2013.

[9] J. Contreras, R. Espinola, F. J. Nogales, and A. J. Conejo, "ARIMA models to predict next-day electricity prices," *IEEE Trans. Power Syst.*, vol. 18, no. 3, pp. 1014–1020, Aug. 2003.

[10] T. Jakasa, I. Androces, and P. Sprcic, "Electricity price forecasting-ARIMA model approach," in *Proc. Int. Conf. Eur. Energy Market (EEM)*, 2011, pp. 222–225.

[11] A. Conejo, M. Plazas, R. Espínola, and A. Molina, "Day-ahead electricity price forecasting using the wavelet transform and ARIMA models," *IEEE Trans. Power Syst.*, vol. 20, no. 2, pp. 1035–1042, May 2005.

[12] J. P. Gonzalez, A. M. S. Roque, and E. A. Perez, "Forecasting functional time series with a new Hilbertian ARMAX model: Application to electricity price forecasting," *IEEE Trans. Power Syst.*, vol. 33, no. 1, pp. 545–556, Jan. 2018.

[13] E. E. Elattar, J. Y. Goulermas, and Q. H. Wu, "Generalized locally weighted GMDH for short term load forecasting," *IEEE Trans. Syst., Man, Cybern. C, Appl. Rev.*, vol. 42, no. 3, pp. 345–356, Mar. 2012.

[14] E. E. Elattar, N. A. Sabiha, M. Alsharef, M. K. Metwaly, A. M. Abd-Elhady, and I. B. M. Taha, "Short term electric load forecasting using hybrid algorithm for smart cities," *Int. J. Speech Technol.*, vol. 50, no. 10, pp. 3379–3399, Oct. 2020.

[15] E. E. Elattar, "Short term wind power prediction using evolutionary optimized local support vector regression," in *Proc. 2nd IEEE PES Int. Conf. Exhib. Innov. Smart Grid Technol.*, Manchester, U.K., Dec. 2011, pp. 1–7.

[16] A. K. Diongue, D. Guégan, and B. Vignal, "Forecasting electricity spot market prices with a K-factor GIGARCH process," *Appl. Energy*, vol. 86, no. 4, pp. 505–510, Apr. 2009.

[17] S. Aggarwal, L. Saini, and A. Kumar, "Electricity price forecasting in Ontario electricity market using wavelet transform in artificial neural network based model," *Int. J. Control Autom. Syst.*, vol. 6, no. 5, pp. 639–650, 2008.

[18] J. P. S. Catalao, S. J. P. S. Mariano, V. M. F. Mendes, and L. A. F. M. Ferreira, "Short-term electricity prices forecasting in a competitive market: A neural network approach," *Electr. Power Syst. Res.*, vol. 77, no. 10, pp. 1297–1304, Aug. 2007.

[19] S. Zhou, L. Zhou, M. Mao, H.-M. Tai, and Y. Wan, "An optimized heterogeneous structure LSTM network for electricity price forecasting," *IEEE Access*, vol. 7, pp. 108161–108173, 2019.

[20] O. Abedinia, N. Amjady, M. Shafie-khah, and J. P. S. Catalao, "Electricity price forecast using combinatorial neural network trained by a new stochastic search method," *Energy Convers. Manage.*, vol. 105, pp. 642–654, Nov. 2015.

[21] N. Amjady and A. Daraeepour, "Mixed price and load forecasting of electricity markets by a new iterative prediction method," *Electr. Power Syst. Res.*, vol. 79, no. 9, pp. 1329–1336, Sep. 2009.

[22] J. Lago, F. De Ridder, and B. De Schutter, "Forecasting spot electricity prices: Deep learning approaches and empirical comparison of traditional algorithms," *Appl. Energy*, vol. 221, pp. 386–405, Jul. 2018.

[23] W. Sun, J.-C. Lu, and M. Meng, "Application of time series based SVM model on next-day electricity price forecasting under deregulated power market," in *Proc. Int. Conf. Mach. Learn. Cybern.*, Shanghai, China, 2006, pp. 2373–2378.

[24] D. Sansom, T. Downs, and T. Saha, "Evaluation of support vector machine based forecasting tool in electricity price forecasting for Australian national electricity market participants," *J. Elect. Electron. Eng.*, vol. 22, no. 3, pp. 227–233, 2003.

[25] X. Yan and N. Chowdhury, "Mid-term electricity market clearing price forecasting: A multiple SVM approach," *Int. J. Elect. Power Energy Syst.*, vol. 58, pp. 206–214, Jun. 2014.

[26] A. Shiri, M. Afshar, A. Rahimi-Kian, and B. Maham, "Electricity price forecasting using support vector machines by considering oil and natural gas price impacts," in *Proc. IEEE Int. Conf. Smart Energy Grid Eng. (SEGE)*, Aug. 2015, pp. 1–5.

[27] M. Kostrzewski and J. Kostrzewska, "Probabilistic electricity price forecasting with Bayesian stochastic volatility models," *Energy Econ.*, vol. 80, pp. 610–620, May 2019.

[28] D. F. Specht, "A general regression neural network," *IEEE Trans. Neural Netw.*, vol. 2, no. 6, pp. 568–576, Dec. 1991.

[29] J. Y. Goulermas, P. Liatsis, and X.-J. Zeng, "Kernel regression networks with local structural information and covariance volume adaptation," *Neurocomputing*, vol. 72, nos. 1–3, pp. 257–261, Dec. 2008.

[30] D.-X. Niu, D. Liu, and M. Xing, "Electricity price forecasting using generalized regression neural network based on principal components analysis," *J. Central South Univ. Technol.*, vol. 15, no. S2, pp. 316–320, Dec. 2008.

[31] A. Pourdaryaei, H. Mokhlis, H. A. Illias, S. H. A. Kaboli, and S. Ahmad, ‘‘Short-term electricity price forecasting via hybrid backtracking search algorithm and ANFIS approach,’’ *IEEE Access*, vol. 7, pp. 77674–77691, 2019.

[32] R. K. Agrawal, F. Muchahary, and M. M. Tripathi, ‘‘Ensemble of relevance vector machines and boosted trees for electricity price forecasting,’’ *Appl. Energy*, vol. 250, pp. 540–548, Sep. 2019.

[33] A. Alshejari, V. S. Kodogiannis, and S. Leonidis, ‘‘Development of neurofuzzy architectures for electricity price forecasting,’’ *Energies*, vol. 13, no. 5, p. 1209, Mar. 2020.

[34] F. Wang, K. Li, L. Zhou, H. Ren, J. Contreras, M. Shafie-Khah, and J. P. S. Cataláo, ‘‘Daily pattern prediction based classification modeling approach for day-ahead electricity price forecasting,’’ *Int. J. Electr. Power Energy Syst.*, vol. 105, pp. 529–540, Feb. 2019.

[35] M. Zahid, F. Ahmed, N. Javaid, R. Abbasi, H. Zainab Kazmi, A. Javaid, M. Bilal, M. Akbar, and M. Ilahi, ‘‘Electricity price and load forecasting using enhanced convolutional neural network and enhanced support vector regression in smart grids,’’ *Electronics*, vol. 8, no. 2, p. 122, Jan. 2019.

[36] J. Wang, F. Liu, Y. Song, and J. Zhao, ‘‘A novel model: Dynamic choice artificial neural network (DCANN) for an electricity price forecasting system,’’ *Appl. Soft Comput.*, vol. 48, pp. 281–297, Nov. 2016.

[37] N. Amjady and F. Keynia, ‘‘Day-ahead price forecasting of electricity markets by mutual information technique and cascaded neuro-evolutionary algorithm,’’ *IEEE Trans. Power Syst.*, vol. 24, no. 1, pp. 306–318, Feb. 2009.

[38] N. Amjady and F. Keynia, ‘‘Day-ahead price forecasting of electricity markets by a new feature selection algorithm and cascaded neural network technique,’’ *Energy Convers. Manage.*, vol. 50, no. 12, pp. 2976–2982, Dec. 2009.

[39] P. Jiang, F. Liu, and Y. Song, ‘‘A hybrid forecasting model based on date-framework strategy and improved feature selection technology for short-term load forecasting,’’ *Energy*, vol. 119, pp. 694–709, Jan. 2017.

[40] (Oct. 2020). *IESO*. [Online]. Available: http://www.ieso.ca/

[41] H. Zareipour, K. Bhattacharya, and C. A. Cañizares, ‘‘Electricity market price volatility: The case of Ontario,’’ *Energy Policy*, vol. 35, no. 9, pp. 4739–4748, Sep. 2007.

[42] F. Takens, *Detecting Strange Attractors in Turbulence* (Lecture Notes in Mathematics), vol. 898. Berlin, Germany: Springer, 1981, pp. 366–381.

[43] T. Sauer, J. A. Yorke, and M. Casdagli, ‘‘Embedology,’’ *J. Stat. Phys.*, vol. 65, nos. 3–4, pp. 579–616, Nov. 1991.

[44] L. Cao, A. Mees, and K. Judd, ‘‘Dynamics from multivariate time series,’’ *Phys. D, Nonlinear Phenomena*, vol. 121, nos. 1–2, pp. 75–88, Oct. 1998.

[45] K. W. Lau and Q. H. Wu, ‘‘Local prediction of non-linear time series using support vector regression,’’ *Pattern Recognit.*, vol. 41, no. 5, pp. 1539–1547, May 2008.

[46] D. Niu, H. Wang, H. Chen, and Y. Liang, ‘‘The general regression neural network based on the fruit fly optimization algorithm and the data inconsistency rate for transmission line icing prediction,’’ *Energies*, vol. 10, no. 12, p. 2066, Dec. 2017.

[47] K. Nose-Filho, A. D. P. Lotufo, and C. R. Minussi, ‘‘Short-term multinodal load forecasting using a modified general regression neural network,’’ *IEEE Trans. Power Del.*, vol. 26, no. 4, pp. 2862–2869, Oct. 2011.

[48] Z. Woo Geem, J. Hoon Kim, and G. V. Loganathan, ‘‘A new heuristic optimization algorithm: Harmony search,’’ *Simulation*, vol. 76, no. 2, pp. 60–68, Feb. 2001.

[49] E. Elattar, ‘‘Combined economic emission dispatch for microgrid considering solar and wind power cost functions using harmony search algorithm,’’ *Int. J. Appl. Eng. Res.*, vol. 13, no. 5, pp. 3083–3092, 2018.

[50] R. Jha, N. K. Meena, A. Swarnkar, N. Gupta, and K. R. Niazi, ‘‘Dynamic economic dispatch of micro-grid using harmony search algorithm,’’ in *Proc. Annu. IEEE India Conf. (INDICON)*, Dec. 2015, pp. 1–6.

[51] H. B. Mann and D. R. Whitney, ‘‘On a test of whether one of two random variables is stochastically larger than the other,’’ *Ann. Math. Statist.*, vol. 18, no. 1, pp. 50–60, Mar. 1947.

[52] F. Wilcoxon, ‘‘Individual comparisons by ranking methods,’’ *Biometrics Bull.*, vol. 1, no. 6, p. 80, Dec. 1945.


**EHAB E. ELATTAR** (Senior Member, IEEE) was born in 1976. He received the B.Sc. (Hons.) and M.Sc. degrees in electrical engineering from the Department of Electrical Engineering, Menoufia University, Egypt, in 1999 and 2003, respectively, and the Ph.D. degree from the Department of Electrical Engineering and Electronics, The University of Liverpool, U.K., in 2010. From 2010 to 2016, he was a Lecturer with the Department of Electrical Engineering, Menoufia University, then he promoted to an Associate Professor, in 2016. He joined the Department of Electrical Engineering, College of Engineering, Taif University, Saudi Arabia. His research interests include power systems analysis and operation, artificial intelligence, modern optimization methods, and its applications to power systems operation and integrating of renewable energy sources into power systems.

**SALAH K. ELSAYED** was born in 1982. He received the B.Sc. (Hons.) and M.Sc. degrees in electrical engineering from the Department of Electrical Engineering, Faculty of Engineering, AL-Azhar University, Cairo, Egypt, in 2005 and 2009, respectively, and the Ph.D. degree from the Department of Electrical Engineering, AL-Azhar University, in 2012. From 2012 to 2017, he was a Lecturer with the Department of Electrical Engineering, AL-Azhar University, then he promoted to an Associate Professor, in 2017. He joined the Department of Electrical Engineering, Faculty of Engineering, Taif University, Saudi Arabia. His research interests include power systems analysis and operation, intelligent systems applications in power systems stability and control, power system optimization techniques, artificial intelligence, and renewable energy sources applications in power systems.

**TAMER AHMED FARRAG** was born in 1981. He received the B.Sc., M.Sc., and Ph.D. degrees from the Department of Computers and Systems Engineering, Mansoura University, Egypt, in 2002, 2006, and 2012, respectively. In Egypt, he worked as an Assistant Professor with the Department of Communications and Computers, MISR Higher Institution of Engineering and Technology. His research interests include artificial intelligence, optimization, programming languages, and computing systems.